Pergamon

Tetrahedron 56 (2000) 5067–5075

TETRAHEDRON

3-Ethyl-6-methyl-isocytosines: Synthesis and Solid State Structural Analysis

Radu Custelcean[a,*] and Liliana Craciun[b,†]

[a]*Department of Chemistry, Michigan State University, East Lansing, MI 48824-1322, USA*
[b]*Department of Organic Chemistry, 'Babes-Bolyai' University, 11 Arany Janos Str., 3400 Cluj-Napoca, Romania*

Received 8 February 2000; accepted 5 April 2000

Abstract—The syntheses and solid state structures of 3-ethyl-6-methyl-5-alkyl-isocytosines (alkyl=H, Me, Et, *n*-Pr, *n*-Bu) are presented. These heterocycles consistently self-assemble into N–H···N hydrogen-bonded dimers, which further associate by N–H···O=C interactions, or N–H···O–H···O=C hydrogen bonds involving water of crystallization, generating extended supramolecular networks. Crystal packing analysis indicates that although hydrogen bonding is the primary intermolecular interaction in these molecular crystals, the dispersion forces may play a decisive role in determining their final three-dimensional arrangements.

The last decade witnessed a spectacular growth of supramolecular synthesis[1–5] and crystal engineering,[6–21] as a result of extensive efforts to exert structural control beyond molecular level, with the ultimate task to build new materials with desired structures and properties.[22–24] This objective proved to be extremely challenging, as the weak forces that govern the organization of molecules in supramolecular structures are difficult to predict and control. In addition, other factors such as molecular symmetry and shape,[14,25] close packing requirement,[26] solvent of crystallization, or kinetics of nucleation,[25] render this problem even more difficult. Until the ab initio calculation of the three dimensional arrangement of molecules in crystals becomes feasible,[27–29] the systematic approach based on the empirical observation of crystal packing changes in response to gradual modifications in molecular structure,[30–35] remains the only practical solution to this problem. When sufficient understanding of intra- and intermolecular interactions, as well as of other pertinent factors is acquired, the successful building of desired supramolecular structures can be eventually accomplished.

Because of their strong ability to self-assemble in extended hydrogen-bonded arrays, heterocycles have been extensively used in supramolecular synthesis.[2,19,36–39] However, due to the high density of hydrogen bonding donors and acceptors present, the prediction of their crystal packing is very often extremely difficult, as numerous hydrogen bonding motifs are usually possible.[40] The isocytosine (2-amino-4-pyrimidinone) system has been recently explored, as a versatile, easily accessible building block for supramolecular synthesis.[40–42] However, the occurrence of two tautomers in solid state has severely limited its applicability to date. For example, isocytosine exhibits both the N1 and the N3 tautomeric forms coexisting in the crystal.[43] The same situation is present in 5-(*p*-chlorophenyl)-6-ethyl-isocytosine.[44] The 6-methyl-isocytosine can be found as two polymorphs, one similar to the one found in the parent ring,[41] and the other containing only the N1 tautomer.[45] This tautomer, on the other hand, is exclusively present in the 6-ethyl and the 6-phenyl derivatives in the solid state.[41] In order to effectively use the isocytosine functionality for crystal engineering, this rather unpredictable tautomerization should be therefore controlled.

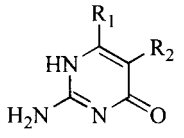

N1

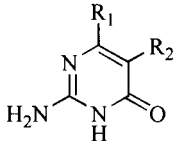

N3

In this paper we describe the synthesis and self-assembly of the 3-ethyl-6-methyl-isocytosines (2-amino-3-ethyl-6-methyl-4(3*H*)-pyrimidinones) **1**–**5** in the solid state. While ethylation at N(3) eliminated the possibility of the above mentioned tautomerization, we hoped that it would also simplify the intermolecular associations by elimination of one H-bonding donor site, making the crystal packing more predictable and therefore easier to control.

Keywords: dispersion interactions; hydrogen bonding; isocytosine; self-assembly.

* Corresponding author. Tel.: +1-517-355-9715, ext. 143; fax: +1-517-353-1793; e-mail: custelce@argus.cem.msu.edu

† Present address: Ciba Specialty Chemicals, West Memphis, AR 72301, USA.

0040–4020/00/$ - see front matter
PII: S0040-4020(00)00288-X

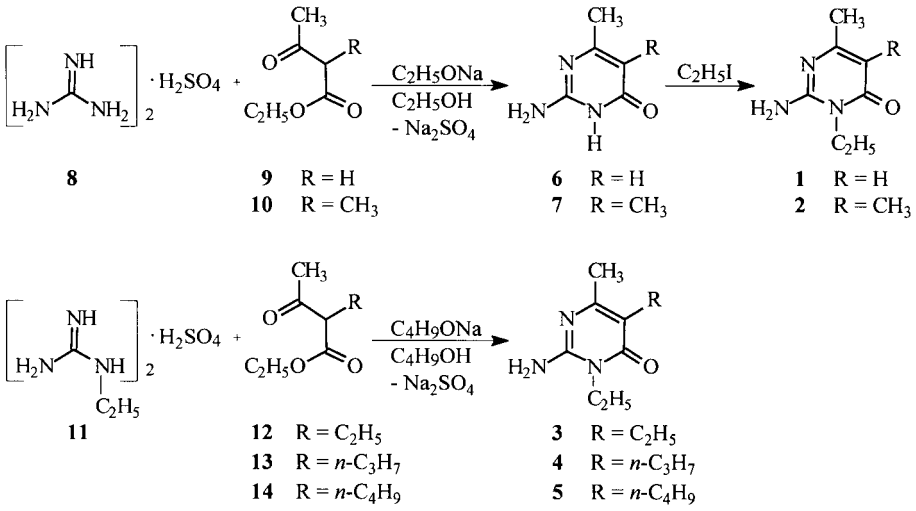

Scheme 1.

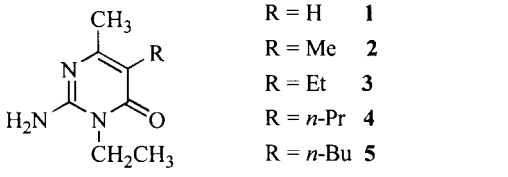

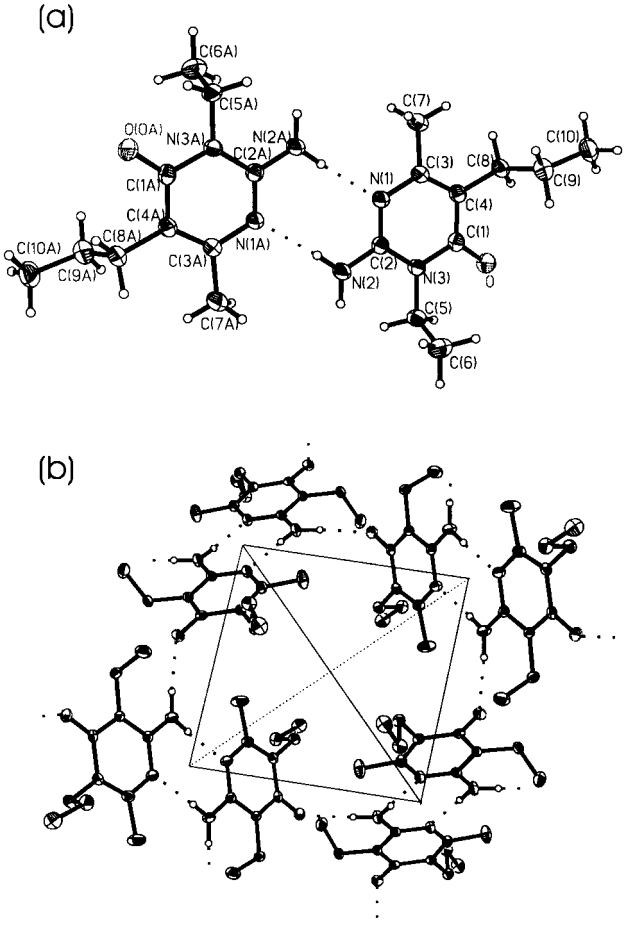

Figure 1. Crystal structure of **4**: (a) self-assembly in dimers. (b) tetrahedral orientation of dimers, linked by N–H···O=C hydrogen bonds.

Results and Discussion

Syntheses

2-Amino-3-ethyl-6-methyl-4(3*H*)-pyrimidinone (**1**) was first isolated by Reznik and Shvetsov as a byproduct of the reaction of 2-amino-6-methyl-4(3*H*)-pyrimidinone (**6**) with paraformaldehyde and triethylphosphite.[46] However, no physical characterization is given for the new compound in this paper. Taran and Raimanova[47] reported the use of compound **1** as an additive that improves the brightness of nickel electrodeposits, but they do not disclose the synthetic route followed to make **1** and once again, no physical characterization is reported. We synthesized **2** in moderate yield by ethylation of **6** with ethyl iodide in a biphasic water–benzene mixture, following a literature method for phase-transfer-catalyzed N-alkylation of amides (Scheme 1).[48] The precursor, compound **6**, was made by condensation of ethyl acetoacetate (**9**) with guanidine sulfate (**8**), following prior reported methodologies.[49–51] The previously unknown 2-amino-3-ethyl-5,6-dimethyl-4(3*H*)-pyrimidinone (**2**) was prepared similarly, by ethylation of 2-amino-5,6-dimethyl-4(3*H*)-pyrimidinone (**7**), which in turn was synthesized from ethyl 2-methylacetoacetate (**10**) and **8**.

To our knowledge, 2-amino-3,5-diethyl-6-methyl-4(3*H*)-pyrimidinone (**3**) and 2-amino-3-ethyl-6-methyl-5-*n*-propyl-4(3*H*)-pyrimidinone (**4**) have not been previously reported in the literature. We prepared compounds **3** and **4** by a method analogous with the reported synthesis of 2-amino-5-*n*-butyl-3-ethyl-6-methyl-4(3*H*)-pyrimidinone (**5**).[52] Thus, **3** and **4** were obtained as byproducts in the condensation of *N*-ethylguanidine sulfate (**11**) with ethyl 2-ethylacetoacetate (**12**) and ethyl 2-*n*-propylacetoacetate (**13**), respectively (Scheme 1). This route failed when applied for compounds **1** and **2**, where condensation of *N*-ethylguanidine with **9** or **10** gave exclusively 2-ethylamino-6-methyl-4(3*H*)-pyrimidinone (**15**) and 2-ethylamino-5,6-dimethyl-4(3*H*)-pyrimidinone (**16**).[53]

Table 1. Hydrogen bonding parameters (Å, °) for **1–5**

D–H···A	D···A	H···A	∠D–H···A
	1		
N(2)–H···N(4)	3.007	2.141	175.1
N(5)–H···N(1)	2.953	2.074	171.5
N(2)–H···O(1)	2.895	2.095	159.7
N(5)–H···O	2.937	2.114	141.8
	2·0.5 H_2O		
N(2)–H···N(1A)	3.019	2.117	172.1
N(2A)–H···N(1)	2.964	2.083	173.1
N(2)–H···O(A)	3.105	2.459	135.5
N(2A)–H···O(B)	2.892	2.037	163.7
O(B)–H···O	2.767	1.922	167.8
O(B)–H···O(A)	2.796	1.960	170.9
	$(3)_{0.77}(4)_{0.23}$·0.5 H_2O		
N(2)–H···N(1A)	2.984	2.191	175.9
N(2A)–H···N(1)	3.001	2.122	173.5
N(2)–H···O(B)	3.161	2.291	165.0
N(2A)–H···O(B)	3.038	2.176	162.0
O(B)–H···O	2.739	1.980	163.7
O(B)–H···O(A)	2.802	1.985	173.2
	4		
N(2)–H···N(1A)	2.987	2.103	176.6
N(2)–H···O	2.925	2.027	169.9
	5[a]		
N–H···N(1)	3.005	2.160	161.8
N–H···O	2.884	2.071	160.7

[a] Ref. 54.

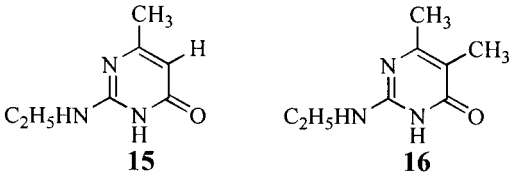

The tautomerism of compounds **1–5** in solution was addressed by NOE experiments. A positive NOE enhancement (2–3%) of the NH_2 signal is observed on irradiation of the exocyclic NCH_2 peak, whereas irradiation of the methyl group in the 6th position shows no effect on the NH_2 ^{1}H NMR signal. These results strongly confirm the prevalence of the amino-oxo forms in solution for **1–5**.

Solid state structural analysis

This study was inspired from the crystal structure of 2-amino-3-ethyl-6-methyl-5-*n*-propyl-4(3*H*)-pyrimidinone (**4**), part of an extensive project investigating the structure-property relationships in isocytosine derivatives.[49–53] The compound crystallized from $CH_3OH/CHCl_3$ in the space group $P4_2/n$, belonging to the tetragonal crystal system. As depicted in Fig. 1, **4** forms centrosymmetric dimers in the solid state, held together by NH···N hydrogen bonds (Table 1), with observed H···N contact distances of 2.103 Å. The dimers are approximately planar, with the C=O groups, however, significantly deviated from the least-squares plane defined by N1, N2, N(1A), N(2A)

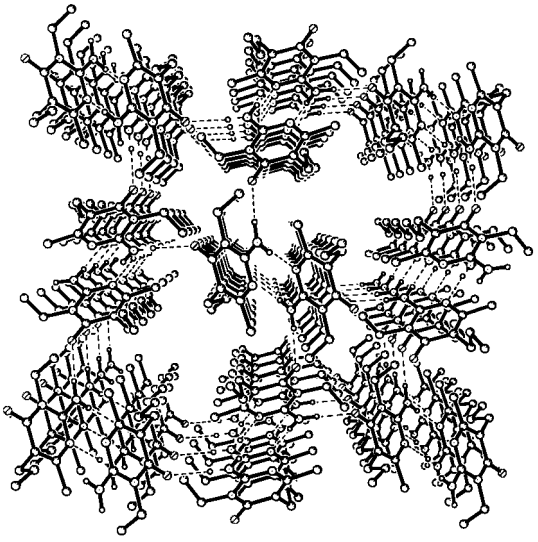

Figure 2. Crystal packing of **4**, viewed along the *c* axis.

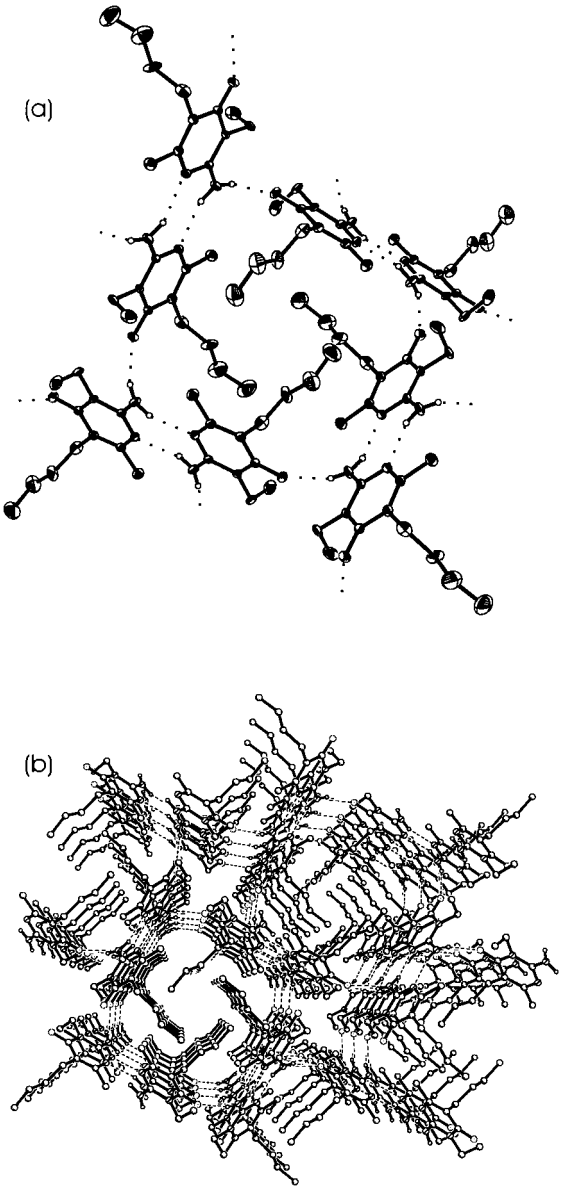

Figure 3. Crystal structure of **5**: (a) hydrogen bonding network; (b) crystal packing viewed along the *c* axis.

(0.159(3) and 0.101(3) Å for O and C1, respectively). These deviations can be explained by the additional hydrogen bonding present, involving the C═O groups and the remaining NH protons, forming a three-dimensional network, with the dimers disposed in a tetrahedral orientation (Fig. 1b), reflecting thus the overall tetragonal symmetry of the crystal. The N–H···O═C contact distances are 2.027 Å long and approximately linear, with the N–H···O angles of 169.9°. The dihedral angle between the least-squares planes (defined by the four N atoms involved in hydrogen bonding) of two adjacent dimers is 70.9°. A closer examination of the crystal packing of **4** (Fig. 2) reveals the presence of infinite channels along the *c* axis, occupied by the hydrophobic propyl chains. Therefore, it appeared to us very appealing the prospect of removing these groups from the isocytosine rings, which would result in a porous structure, provided the crystal packing remains the same. The previously determined crystal structure of **5** was encouraging, as it adopts the same packing as **4** (Fig. 3), with a slightly bigger unit cell, as expected due to the extra methylene group.[54] This fact suggested that the three-dimensional hydrogen bonding network found in **4** might be robust enough to tolerate even more profound structural modifications in the 5-alkyl chain. We therefore synthesized the 2-amino-3-ethyl-6-methyl-4(3*H*)-pyrimidinone (**1**) and determined its crystal structure. Like **4**, **1** associates into hydrogen-bonded dimers in solid state (Fig. 4). However, no center of symmetry relates the two isocytosine rings, as both ethyl groups are oriented on the same side of the dimer's plane. The two NH···N hydrogen bonds (Table 1) are also slightly different, with H···N contact distances of 2.074 and 2.141 Å, respectively. The planarity of the dimers is more severely distorted than in **4**, with the largest deviations from the least-squares plane defined by N1, N2, N4 and N5 as big as 0.659(3) and 0.448(2) Å for O(1) and C(9), respectively. Further N–H···O═C hydrogen bonds (Table 1) link the dimers (Fig. 4b), with H···O contact distances of 2.095 and 2.114 Å. The dihedral angle of 71.1° between adjacent dimers is very similar to the corresponding value in **4**. However, despite the similar appearance, the crystal packings of **1** and **4** are significantly different. Fig. 5 shows the relationship between the two H-bonding motifs, A and B, interrelated by 180° out-of-plane rotation of half of the dimers, and gliding. This interconversion might occur during the molecular recognition process accompanying nucleation. In the absence of the 5-alkyl groups, the more compact motif B is eventually preferred, leading thus to a more efficient packing in **1**, which unfortunately precludes the formation of the desired porous solid. Instead, two-dimensional hydrogen-bonded corrugated sheets are formed, self-assembled into bilayers, with all *N*-Et groups pointing inward, which presumably optimizes their van der Waals interactions (Fig. 6). The contribution of these weak forces to the overall lattice energy is probably small compared to the corresponding energy of the much stronger hydrogen bonds. Nevertheless, under the present circumstances, with the two H-bonding motifs seemingly equally favored, the dispersion interactions become decisive in determining the final three-dimensional crystal packing.[55] Attempts to enforce the H-bonding motif A by using different hydrocarbons such as hexane, heptane, methylcyclohexane or benzene, as potential templates that might compensate the absence of the 5-*n*-propyl or 5-*n*-butyl groups, were unsuccessful to date.

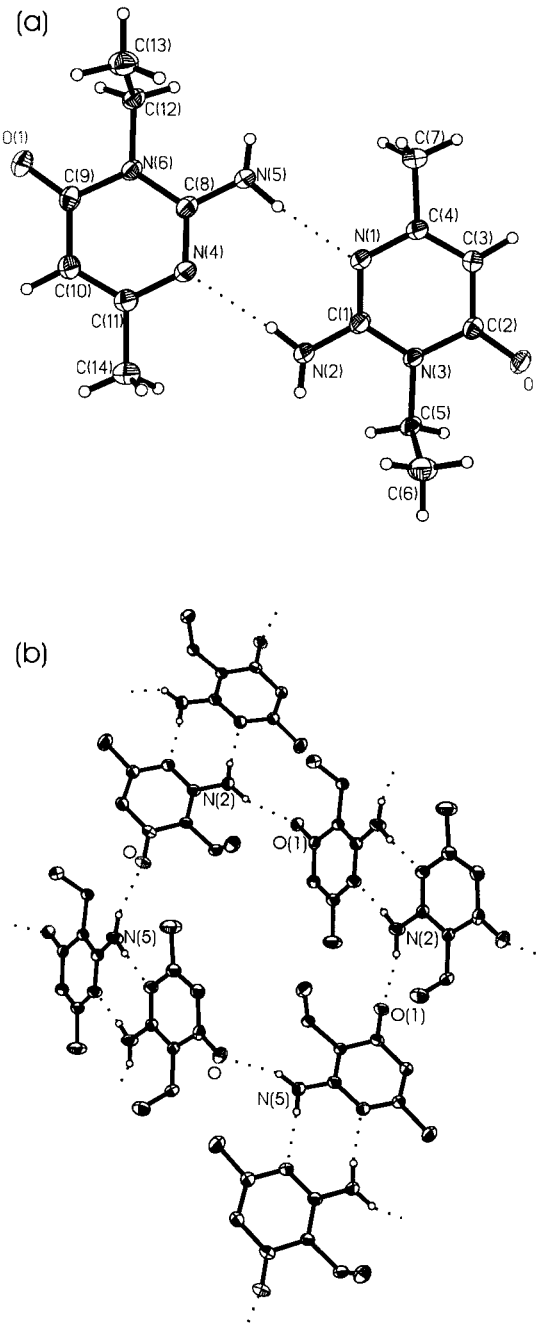

Figure 4. Crystal structure of **1**: (a) self-assembly in dimers; (b) hydrogen bonding network.

Having defined the two limits of the series, we naturally became interested to find out the transition point between the two crystal packings, or to possibly identify other H-bonding motifs. We therefore synthesized the 5-Me (**2**) and 5-Et (**3**) derivatives, and pursued their solid state structural investigations. The 2-amino-3-ethyl-5,6-dimethyl-4(3*H*)-pyrimidinone (**2**) crystallized from THF with 0.5 mol of H_2O, as revealed by X-ray analysis. Attempts to crystallize it free of water, by using different solvents, were unsuccessful to date. Nevertheless, **2** exhibits

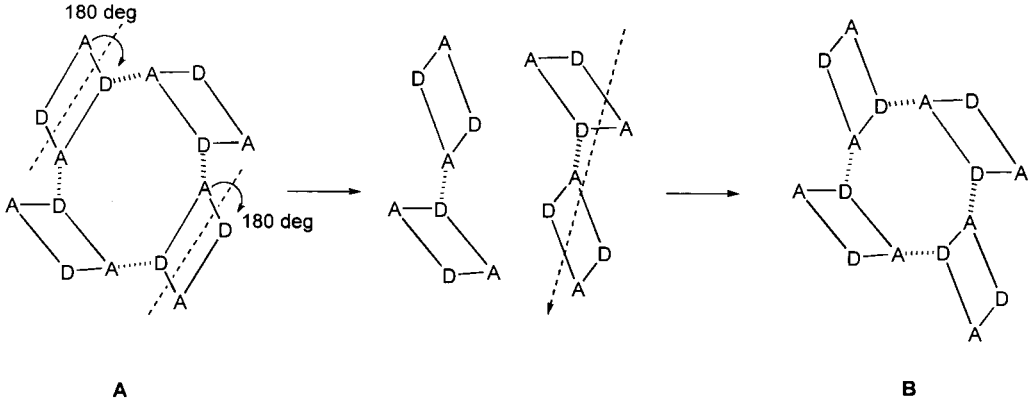

Figure 5. Schematic representation of the relationship between the hydrogen bonding motifs in **4**–**5** (A) and **1** (B).

the same association in dimers that was observed in the previous structures (Fig. 7). However, the isocytosine rings are significantly twisted relative to each other, with a dihedral angle between the planes defined by the nitrogen atoms in each ring, of 31.2°. The water of crystallization interconnects the dimers by participating to two O–H···O═C interactions as a H-bonding donor, and as an acceptor in a N–H···OH hydrogen bond (Fig. 7b). The remaining N(2)–H, however, prefers to interact with the C═O(A) carbonyl group, in a weaker hydrogen bond (Table 1). The result is a complex three-dimensional H-bonding network.

Similarly, **3** crystallized with 0.5 mol of H_2O. The X-ray analysis of this compound, also revealed the presence of **4** in the crystal, as a result of accidental contamination. The extra C atoms in the two unique isocytosine rings were refined with the partial occupancy of 0.254 and 0.211, estimating thus the proportion of the 5-*n*-Pr derivative around 23%. ^{1}H NMR analysis confirmed the presence of about 20–25% of **4** in the sample used for the X-ray investigation. The rest of the atoms corresponding to the two structures are not distinguishable, the only effect of the disorder being a slight increase in the displacement parameters, especially for the C atoms in the alkyl chains. Once again, the isocytosine rings associate into N–H···N hydrogen bonded dimers (Fig. 8), that, however, are severely deviated from planarity, exhibiting a dihedral angle between

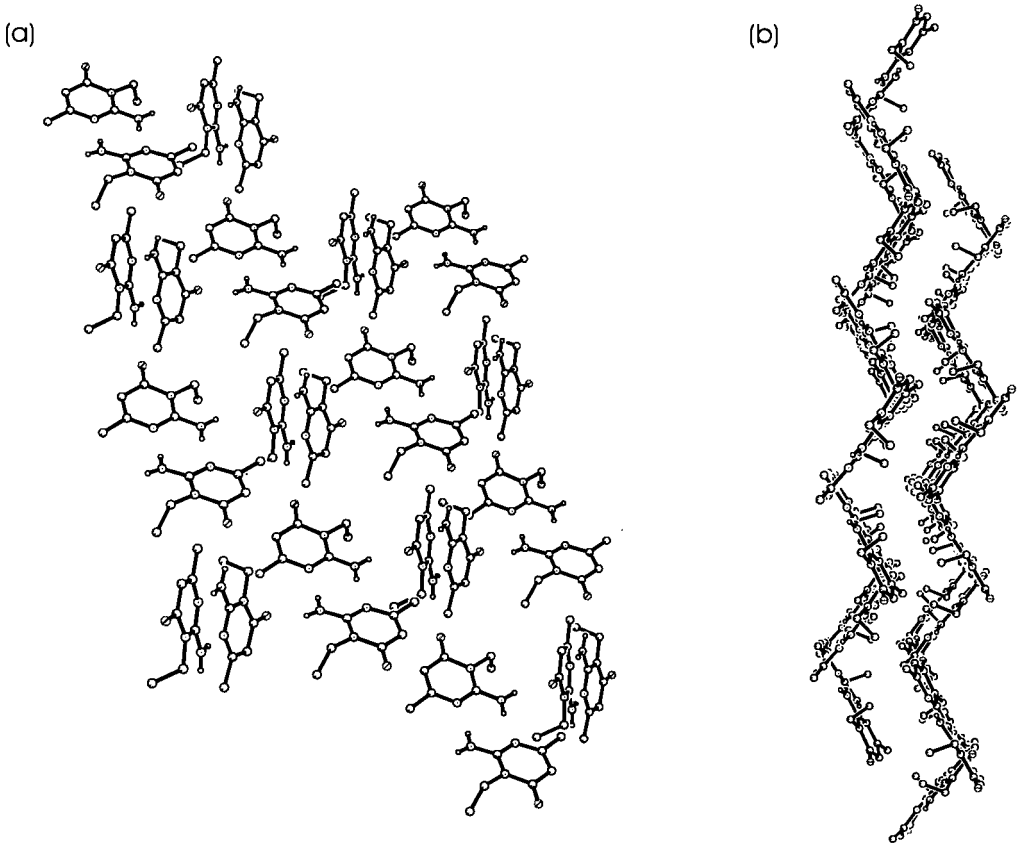

Figure 6. Crystal packing of **1**: (a) hydrogen-bonded corrugated sheet; (b) self-assembly in bilayers.

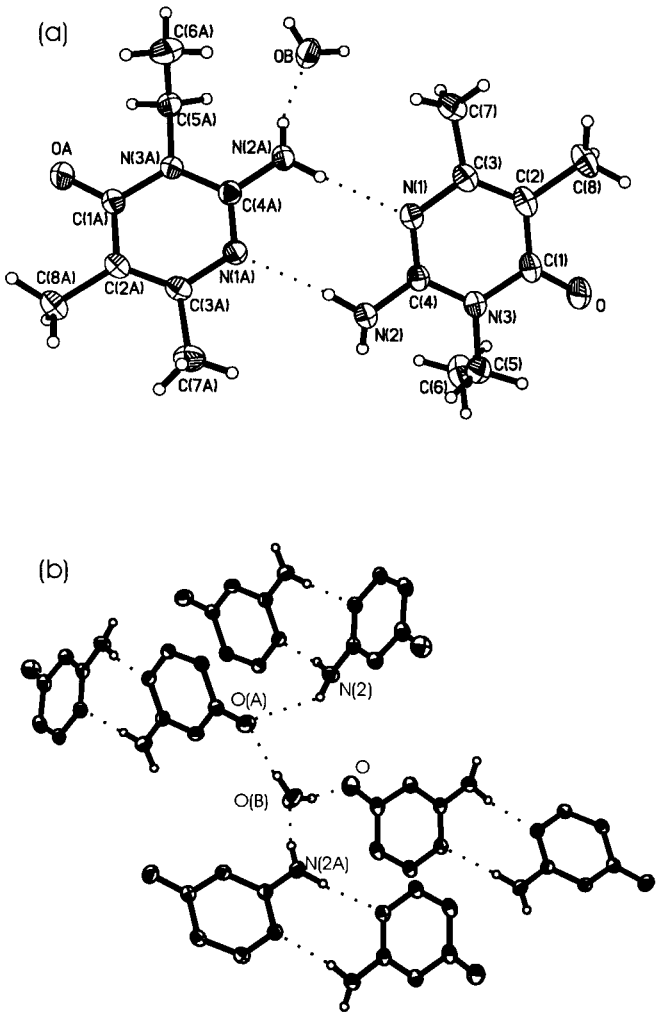

Figure 7. Crystal structure of **2**·0.5 H_2O: (a) self-assembly in dimers; (b) hydrogen bonding network involving water of crystallization (alkyl groups not shown for clarity).

the planes defined by the N atoms, of 46.8°. The water molecules play both the role of donors and acceptors in O–H···O═C and N–H···OH interactions (Table 1), respectively, linking the dimers in a three-dimensional H-bonding network (Fig. 8b).

Conclusions

3-Et-6-Me-isocytosines **1**–**5** consistently self-assemble into N–H···N hydrogen bonded dimers in the solid state. Moreover, the dimers can further associate by N–H···O═C hydrogen bonds into extended supramolecular arrays. However, the presence of water of crystallization can disrupt this H-bonding motif, as illustrated by the crystal structures of **2**·0.5 H_2O and $(\mathbf{3})_{0.76}(\mathbf{4})_{0.23}$·0.5 H_2O. In these hydrates, the water molecules link the dimers by O–H···O═C and N–H···OH hydrogen bonds, into three-dimensional hydrogen-bonded networks. The significantly different packing arrangements of **4**–**5** and **1** emphasize once again the difficulties associated with the ab initio prediction of the three-dimensional organization of molecules in crystals. While **4** and **5** form 3-D hydrogen bonding networks, a similar packing in **1** would have resulted in a porous molecular crystal. However, while adopting a very similar H-bonding motif, **1** found an alternative arrangement into 2-D sheets, self-assembled into bilayers, leading to a more effective crystal packing, which presumably optimized the dispersion interactions of the *N*-Et chains. Thus, although hydrogen bonding is the dominant intermolecular interaction in these crystals, it appears that the cooperative effect of the dispersion forces makes a significant contribution to the overall lattice energy, decisively influencing the three-dimensional crystal packing.

Experimental

Solvents were distilled and/or stored over 4 Å molecular sieves prior to use. All other reagents were used as obtained from commercial sources or purified according to standard procedures. Experimental yields were not optimized. Melting points were determined in sealed capillaries on a Thomas Hoover Unimelt apparatus, and are uncorrected. Proton (^{1}H) and carbon (^{13}C) NMR spectra were measured at ambient temperature on a Varian 500 MHz spectrometer, and were referenced to solvent signals. Infrared spectra

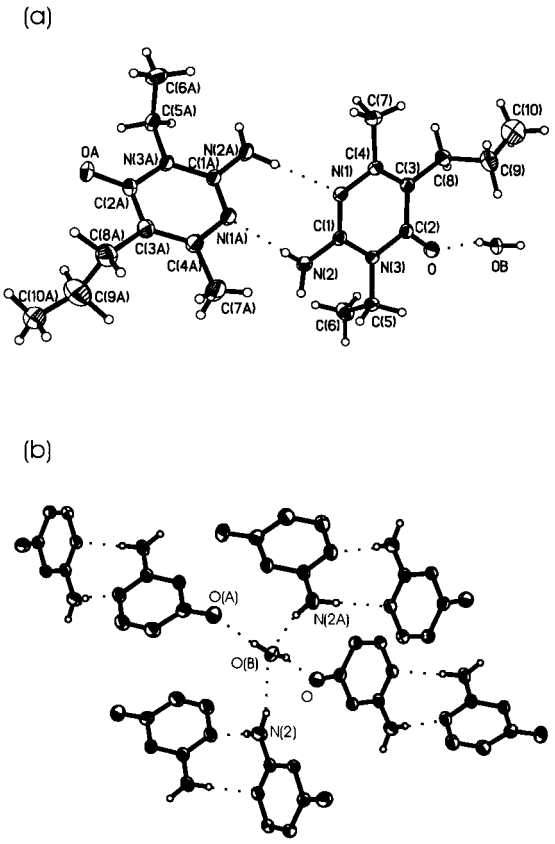

Figure 8. Crystal structure of $(\mathbf{3})_{0.76}(\mathbf{4})_{0.23}{\cdot}0.5\ H_2O$: (a) self-assembly in dimers; (b) hydrogen bonding network involving water of crystallization (alkyl groups not shown for clarity).

were recorded on a Nicolet 730 FT-IR spectrophotometer. GC/MS analyses were carried out on a Hewlett-Packard 5890/5971 gas chromatograph-mass selective detector.

2-Amino-3-ethyl-6-methyl-4(3*H*)-pyrimidinone (1) and 2-amino-3-ethyl-5,6-dimethyl-4(3*H*)-pyrimidinone (2). A solution of ethyl iodide (650 mg, 4.2 mmol) in benzene was added dropwise with efficient stirring to the refluxing mixture of 2-amino-6-methyl-4(3*H*)-pyrimidinone **6** or **7** (2.7 mmol), finely powdered potassium hydroxide (550 mg), potassium carbonate (750 mg), tetra-*n*-butylammonium hydrogen sulfate (91 mg), and benzene (10 mL). Stirring was continued for 4 h at reflux. The resultant mixture was cooled to room temperature, treated with water, and extracted with chloroform. The organic phase was separated, washed with water, dried over anhydrous magnesium sulfate, and evaporated to give a white solid. Recrystallization from ethanol gave 2-amino-3-ethyl-6-methyl-4(3*H*)-pyrimidinone (**1**) in 15% yield, and 2-amino-3-ethyl-5,6-dimethyl-4(3*H*)-pyrimidinone (**2**) in 28% yield.

2-Amino-3,5-diethyl-6-methyl-4(3*H*)-pyrimidinone (3), and 2-amino-3-ethyl-6-methyl-5-*n*-propyl-4(3*H*)-pyrimidinone (4). To a stirred solution of sodium *n*-butoxide (11 mmol) in anhydrous *n*-butanol (100 mL) was added 1.5 g of *N*-ethylguanidine sulfate **11** (5.5 mmol) and the mixture was refluxed for 30 min, cooled in an ice bath and filtered. Ethyl 2-alkylacetoacetate (freshly distilled; 11 mmol) **12** or **13**, was added dropwise to the filtrate under stirring, and the reaction mixture was refluxed for 12 h. After cooling, water was added and the reaction mixture was made strongly basic with 25% aqueous NaOH. Filtration, followed by recrystallization of the white solid from CH_3NO_2 gave **3** or **4** in yields of 27 and 22%, respectively.

2-Amino-3-ethyl-6-methyl-4(3*H*)-pyrimidinone (1) was obtained as white crystals with mp 223–224°C; ^{1}H NMR ($CDCl_3$) δ 5.80 (s, 1H), 5.18 (s, broad, 1H, exchangeable), 4.00 (q, J=7.3 Hz, 2H), 2.12 (s, 3H), 1.33 (t, J=7.3 Hz, 3H); ^{13}C NMR ($CDCl_3$) δ 163.32 (C(4)), 162.32 (C(2)), 154.06 (C(6)), 103.01 (C(5)), 36.70 (NCH_2CH_3), 23.60 (NCH_2CH_3), 12.67 (CH_3); IR (KBr) ν_{max} 3351, 3156, 3086, 2985, 1692, 1657 (s), 1521 (s), 1491, 1452, 1427, 1452, 1188, 1146, 1016, 810, 786 cm^{-1}; MS (EI) *m/z* for $C_7H_{11}N_3O$ 153 (M^+, 15), 138 (61), 125 (481), 109 (100), 97 (100), 84 (35), 82 (31), 69 (36), 67 (36), 54 (37). Single crystals suitable for X-ray analysis were grown by slow evaporation from chloroform–acetone.

2-Amino-3-ethyl-5,6-dimethyl-4(3*H*)-pyrimidinone (2) was obtained as white crystals with mp 176–178°C; ^{1}H NMR ($CDCl_3$) δ 4.73 (s, broad, 1H, exchangeable), 4.01 (q, J=7.3 Hz, 2H), 2.15 (s, 3H), 1.98 (s, 3H), 1.33 (t, J=7.3 Hz, 3H); ^{13}C NMR ($CDCl_3$) δ 161.84 (C(4)), 159.00 (C(2)), 152.53 (C(6)), 105.04 (C(5)), 35.85 (NCH_2CH_3), 21.45 (NCH_2CH_3), 12.49 (C(6)CH_3), 11.10 (C(5)CH_3); IR (KBr) ν_{max} 3390, 3348, 3153, 3117, 2982, 2940, 1681, 1639 (s), 1536 (s), 1502, 1456, 1209, 1131, 979, 791 cm^{-1}; MS (EI) *m/z* for $C_8H_{13}N_3O$ 167 (M^+, 28), 139 (100), 138 (53), 124 (21), 111 (59), 110 (51), 96 (28), 69 (31), 55 (27), 53 (28). Single crystals suitable for X-ray analysis were grown by slow evaporation from THF.

2-Amino-3,5-diethyl-6-methyl-4(3*H*)-pyrimidinone (3) was obtained as white needle crystals with mp 172–173°C; ^{1}H NMR ($CDCl_3$) δ 11.35 (s, broad, 1H, exchangeable), 4.00 (q, J=7.3 Hz, 2H, NCH_2CH_3), 2.45 (q, J=7.3 Hz, 2H, CH_2CH_3), 2.15 (s, 3H), 1.32 (t, J=7.3 Hz, 3H, NCH_2CH_3), 1.06 (t, J=7.3 Hz, 3H, CH_2CH_3); ^{13}C NMR ($CDCl_3$) δ 161.97 (C(4)), 157.87 (C(2)), 151.66 (C(6)), 115.63 (C(5)), 36.95 (NCH_2CH_3), 20.74 (NCH_2CH_3), 19.34 (CH_2CH_3), 13.13 (CH_2CH_3), 12.53 (CH_3); IR (KBr) ν_{max} 3421, 3340, 3144, 3099, 2976, 2929, 1669, 1625 (s), 1524 (s), 1444, 1410, 1318, 1198, 792 cm^{-1}; MS (EI) *m/z* for $C_9H_{15}N_3O$ 181 (M^+, 33), 166 (100), 150 (25), 138 (70), 110 (10), 96 (32), 69 (10). Single crystals suitable for X-ray analysis were grown by slow evaporation from chloroform–acetone.

2-Amino-3-ethyl-6-methyl-5-*n*-propyl-4(3*H*)-pyrimidinone (4) was obtained as white needle crystals with mp 193–194°C; ^{1}H NMR ($CDCl_3$) δ 5.43 (s, broad, 1H, exchangeable), 3.99 (q, J=7.3 Hz, 2H, NCH_2CH_3), 2.39 (t, J=7.3 Hz, 2H, $CH_2CH_2CH_3$), 2.13 (s, 3H), 1.44 (sextet, J=7.3 Hz, 2H, $CH_2CH_2CH_3$), 1.31 (t, J=7.3 Hz, 3H, NCH_2CH_3), 0.91 (t, J=7.3 Hz, 3H, $CH_2CH_2CH_3$); ^{13}C NMR ($CDCl_3$) δ 162.26 (C(4)), 158.58 (C(2)), 151.88 (C(6)), 113.96 (C(5)), 36.87 (NCH_2CH_3), 28.12 ($CH_2CH_2CH_3$), 22.03 ($CH_2CH_2CH_3$), 21.05 (NCH_2CH_3), 14.11 ($CH_2CH_2CH_3$), 12.49 (CH_3); IR (KBr) ν_{max} 3370, 3343, 3145, 3109, 2959, 2932, 1683, 1631

Table 2. Crystallographic data for **1–4**

	1	2·$(H_2O)_{0.5}$	$(3)_{0.77}(4)_{0.23}$·$(H_2O)_{0.5}$	4
Formula	$C_7H_{11}N_3O$	$C_8H_{14}N_3O_{1.5}$	$C_{9.23}H_{16.46}N_3O_{1.5}$	$C_{10}H_{17}N_3O$
Formula weight	153.19	176.22	193.47	195.27
Dimensions, mm	0.41×0.36×0.10	0.60×0.57×0.18	0.60×0.49×0.08	0.44×0.34×0.26
Crystal system	Monoclinic	Monoclinic	Monoclinic	Tetragonal
Space group, Z	$P2_1/n$, 8	$P2_1/n$, 8	$P2_1/n$, 8	$P4_2/n$, 8
a, Å	12.1028(5)	11.7406(6)	14.3955(2)	16.4048(4)
b, Å	10.3188(4)	8.7183(4)	9.2865(1)	16.4048(4)
c, Å	12.7922(5)	19.0055(9)	17.57120(10)	8.5052(3)
α, deg	90	90	90	90
β, deg	97.7500(10)	105.9080(10)	114.0320(10)	90
γ, deg	90	90	90	90
V, Å^3	1582.98(11)	1870.86(16)	2145.37(3)	2288.90(11)
Temperature, K	173	173	173	173
d_{calcd}, g/cm^{-3}	1.286	1.251	1.198	1.133
Reflections collected	9667	10894	12759	7148
Unique reflections	3704	4313	4918	2376
$2\theta_{max}$, deg	28.30	28.27	28.19	27.49
No. of parameters	287	339	381	196
R_1[a], wR_2[b] ($I>2\sigma$)	0.0390, 0.1026	0.0417, 0.1181	0.0640, 0.1565	0.0386, 0.0965
R_1, wR_2 (all data)	0.0508, 0.1090	0.0540, 0.1263	0.0887, 0.1732	0.0569, 0.1043
Goodness of fit	1.029	1.038	1.020	1.047

[a] $R_1 = \sum(|F_0| - |F_c|)/\sum|F_0|$.
[b] $wR_2 = \{\sum[W(F_0^2 - F_c^2)^2]/\sum[w(F_0^2)^2]\}^{1/2}$

(s), 1524 (s), 1443, 1409, 1198, 1126, 792 cm^{-1}; MS (EI) m/z for $C_{10}H_{17}N_3O$ 195 (M^+, 11), 167 (11), 166 (100), 138 (28), 96 (19). Single crystals suitable for X-ray analysis were grown by slow evaporation from chloroform–methanol.

X-Ray crystal structure determination of 1–4. X-Ray crystallographic measurements (Table 2) were carried out on a Siemens SMART CCD diffractometer with graphite-monochromated Mo Kα radiation (λ=0.71073 Å), operated at 50 kV and 40 mA. The structures were solved by direct methods and refined on F^2 using the SHELXTL software package.[56] Absorption corrections were applied using SADABS, part of the SHELXTL software package. All non-hydrogen atoms were refined anisotropically. Hydrogen atoms were located from difference Fourier maps and refined isotropically, except for the methyl hydrogens from the propyl groups of **4**, in $(\mathbf{3})_{0.76}(\mathbf{4})_{0.23}$·0.5 H_2O, which were calculated and placed in idealized positions.

Acknowledgements

R. C. gratefully acknowledges his advisor, Professor James E. Jackson (MSU), for promoting intellectual independence and a stimulating and creative ambience in his research group, without which this project would have never been possible.

References

1. Lehn, J.-M. *Angew. Chem. Int. Ed.* **1990**, *29*, 1304–1319.
2. Whitesides, G. M.; Simanek, E. E.; Mathias, J. P.; Seto, C. T.; Chin, D. N.; Hammen, M.; Gordon, D. M. *Acc. Chem. Res.* **1995**, *28*, 37–44.
3. Yaghi, O. M.; Li, H.; Davis, C.; Richardson, D.; Groy, T. L. *Acc. Chem. Res.* **1998**, *31*, 474–484.
4. Stang, P. J.; Olenyuk, B. *Acc. Chem. Res.* **1997**, *30*, 502–518.
5. Fyfe, M. C. T.; Stoddart, F. *Coord. Chem. Rev.* **1999**, *18*, 139–155.
6. Desiraju, G. R. *Angew. Chem. Int. Ed.* **1995**, *34*, 2311–2327.
7. Desiraju, G. R. *Chem. Commun.* **1997**, 1475–1482.
8. MacDonald, J. C.; Whitesides, G. M. *Chem. Rev.* **1994**, *94*, 2383–2420.
9. Ermer, O.; Eling, A. *J. Chem. Soc., Perkin Trans. 2* **1994**, 925–944.
10. Subramanian, S.; Zaworotko, M. J. *Coord. Chem. Rev.* **1994**, *137*, 357–401.
11. Aakeroy, C. B. *Acta. Cryst.* **1997**, *B53*, 569–586.
12. Braga, D.; Grepioni, F. *Coord. Chem. Rev.* **1999**, *183*, 19–41.
13. Blake, A. J.; Champness, N. R.; Hubberstey, P.; Li, W.-S.; Withersby, A.; Schroder, M. *Coord. Chem. Rev.* **1999**, *183*, 117–138.
14. Chang, Y.-L.; West, M.-A.; Fowler, F. W.; Lauher, J. W. *J. Am. Chem. Soc.* **1993**, *11*, 5991–6000.
15. Hoskins, B. F.; Robson, R. *J. Am. Chem. Soc.* **1990**, *112*, 1546–1554.
16. Aoyama, Y.; Endo, K.; Anzai, T.; Yamaguchi, Y.; Sawaki, T.; Kobayashi, K.; Kanehisa, N.; Hashimoto, H.; Kai, Y.; Masuda, H. *J. Am. Chem. Soc.* **1996**, *118*, 5562–5571.
17. Wang, X.; Simard, M.; Wuest, J. D. *J. Am. Chem. Soc.* **1994**, *116*, 12119–12120.
18. Russel, V. A.; Evans, C. C.; Li, W.; Ward, M. D. *Science* **1997**, *276*, 575–579.
19. Fan, E.; Vicent, C.; Geib, S. J.; Hamilton, A. D. *Chem. Mater.* **1994**, *6*, 1113–1117.
20. Bishop, R. *Chem. Soc. Rev.* **1996**, 311–319.
21. Biradha, K.; Dennis, D.; MacKinnon, V. A.; Sharma, C. V. K.; Zaworotko, M. J. *J. Am. Chem. Soc.* **1998**, *120*, 11894–11903.
22. Alivisatos, A. P.; Barbara, P. F.; Castleman, A. W.; Chang, J.; Dixon, D. A.; Klein, M. L.; McLendon, G. L.; Miller, J. S.; Ratner, M. A.; Rossky, P. J.; Stupp, S. I.; Thompson, M. E. *Adv. Mater.* **1998**, *10*, 1297–1336.

23. Muthuraman, M.; Le Fur, Y.; Bagieu-Beucher, M.; Masse, R.; Nicoud, J.-F.; Desiraju, G. R. *J. Mater. Chem.* **1999**, *9*, 2233–2239.
24. Langley, P. J.; Hullinger, J. *Chem. Soc. Rev.* **1999**, *28*, 279–292.
25. Brock, C. P.; Dunitz, J. D. *Chem. Mater.* **1994**, *6*, 1118–1127.
26. Kitaigorodskii, A. I. *Organic Chemical Crystallography*; Consultant's Bureau: New York, 1961.
27. Maddox, J. *Nature* **1988**, *335*, 201.
28. Gavezzotti, A. *Acc. Chem. Res.* **1994**, *27*, 309–314.
29. Wolff, J. J. *Angew. Chem. Int. Ed.* **1996**, *35*, 2195–2197.
30. Leiserowitz, L. *Acta Cryst.* **1976**, *B32*, 775–802.
31. Leiserowitz, L. *Acta Cryst.* **1978**, *B34*, 1230–1247.
32. Garcia-Tellado, F.; Geib, S. J.; Goswami, S.; Hamilton, A. D. *J. Am. Chem. Soc.* **1991**, *113*, 9265–9269.
33. Lin, Q.; Geib, S. J.; Hamilton, A. D. *J. Chem. Soc., Perkin Trans. 2* **1998**, 2109–2116.
34. Aakeroy, C. B.; Nieuwenhuyzen, M. *J. Am. Chem. Soc.* **1994**, *116*, 10983–10991.
35. Kolotuchin, S. V.; Thiessen, P. A.; Fenlon, E. E.; Wilson, S. R.; Loweth, C. J.; Zimmerman, S. C. *Chem. Eur. J.* **1999**, *5*, 2537–2547.
36. Russell, K. C.; Lehn, J.-M.; Kyritsakas, N.; DeCian, A.; Fischer, J. *New J. Chem.* **1998**, 123–128.
37. Kolotuchin, S. V.; Zimmerman, S. C. *J. Am. Chem. Soc.* **1998**, *120*, 9092–9093.
38. Brunet, P.; Simard, M.; Wuest, J. D. *J. Am. Chem. Soc.* **1997**, *119*, 2737–2738.
39. Vaillancourt, L.; Simard, M.; Wuest, J. D. *J. Org. Chem.* **1998**, *63*, 9746–9752.
40. Liao, R.-F.; Lauher, J. W.; Fowler, F. W. *Tetrahedron* **1996**, *52*, 3153–3162.
41. Toledo, L. M.; Musa, K.; Lauher, J. W.; Fowler, F. W. *Chem. Mater.* **1995**, *7*, 1639–1647.
42. Beijer, F. H.; Sijbesma, R. P.; Kooijman, H.; Speck, A. L.; Meijer, E. W. *J. Am. Chem. Soc.* **1998**, *120*, 6761–6769.
43. Sharma, B. D.; McConnell, J. F. *Acta Cryst.* **1965**, *19*, 797–806.
44. Griffin, R. J.; Schwalbe, C. H.; Stevens, M. F. G.; Wong, K. P. *J. Chem. Soc., Perkin Trans. 1* **1985**, 2267–2276.
45. Lowe, P. R.; Schwalbe, C. H. *Acta Cryst.* **1987**, *C43*, 330–333.
46. Reznik, V. S.; Shvetsov, Y. S. *Izv. Acad. Nauk SSSR, Ser. Khim.* **1975**, *24*, 385.
47. Taran, L. A.; Raimanova, T. I. *Zashch. Met.* **1990**, *26* (3), 483.
48. Koziara, A.; Zawadzki, S.; Swierzak, A. *Synthesis* **1979**, 527.
49. Craciun, L.; Horvath, A.; Mager, S. *Studia Univ. Babes-Bolyai, Chem.* **1996**, *41*, 35.
50. Craciun, L.; Kovacs, D.; Craciun, R.; Mager, S. *Heterocycl. Commun.* **1998**, *4*, 157–162.
51. Craciun, L.; Custelcean, R.; Mager, S. *Struct. Chem.* **1999**, *10*, 303–310.
52. Mager, S.; Cristea, I.; Craciun, L.; Irimie, F.; Diudea, M. *Rev. Roum. Chim.* **1991**, *36*, 665–670.
53. Craciun, L.; Custelcean, R. Manuscript in preparation.
54. Craciun, L.; Huang, R.; Mager, S. *Monatsh. Chem.* **1998**, *129*, 735–740.
55. For the importance of the dispersion interactions in determining the lattice energy see: (a) Stone, A. J.; Tsuzuki, S. *J. Phys. Chem. B* **1997**, *101*, 10178–10183. (b) Dunitz, J. D.; Gavezzotti, A. *Acc. Chem. Res.* **1999**, *32*, 677–684.
56. SHELXTL: *Structure Analysis Program 5.1*; Bruker AXS, Inc., Madison, WI, 1997.